

1 **Highlights**

- 2 • Whole-cell bioreporter based on *recA* promoter and GFP reporter was developed for
- 3 formaldehyde bio-sensing
- 4 • Bioreporter cells were immobilized in calcium-alginate hydrogel beads
- 5 • The assay solution effect was shown to improve sensitivity of alginate beads for gas phase
- 6 experiments
- 7 • The detection limits of bead immobilized bioreporter for liquid and gaseous formaldehyde
- 8 were 7.5 µg/mL and 8.1 ppm, respectively

9

10 **Formaldehyde Sensing in Air and Water Using**

11 **Fluorescent Bacterial Bioreporter Cells**

12 Evrim Elcin¹, Ferhan Ayaydin^{2,3}, Huseyin Avni Öktem^{*4,5}

13

14 ¹ Adnan Menderes University, Department of Agricultural Biotechnology, 09970, Aydın, Turkey

15 ² Hungarian Centre of Excellence for Molecular Medicine (HCMM) Nonprofit Ltd, Szeged, Hungary

16 ³ Laboratory of Cellular Imaging, Biological Research Centre, Eötvös Loránd Research Network, Szeged, Hungary

17 ⁴ Middle East Technical University, Department of Biological Sciences, 06800, Ankara, Turkey

18 ⁵ Nanobiz Technology Inc. Gallium Block: 27/218, METU-Science Park, 06800, Ankara, Turkey

19

20 * Corresponding Author: Hüseyin Avni Öktem

21 E-mail addresses: haoktem@metu.edu.tr (H. A. Öktem), ferhan.ayaydin@hceimm.eu

22 (F. Ayaydin), e.elcin@adu.edu.tr (E. Elcin)

23 Phone: +90 532 3956668 (H.A. Öktem)

24 ORCID ID

25 <https://orcid.org/0000-0002-5860-8807> (E. Elcin)

26 <https://orcid.org/0000-0002-1009-9820> (H. A. Öktem)

27
28
29
30
31
32
33
34
35
36
37
38
39
40
41
42
43
44
45
46
47
48
49
50
51
52
53

Abstract

Formaldehyde is a genotoxic volatile organic pollutant and one of the causative agents of sick building syndrome. Despite of its hazardous carcinogenic effects, it has been still used in daily life products and household materials. Hence, determination of formaldehyde in ambient air and drinking water sources is crucial to prevent its adverse health effects. Whole-cell biosensors have emerged as bio-sentinels for environmental monitoring to assess pollution in air, water, and soil. Herein whole-cell bacterial bioreporter was developed based on a DNA damage response gene promoter and green fluorescent reporter protein, and the cells were entrapped in calcium-alginate hydrogel beads for sensitive detection of formaldehyde in air and water. Alginate bead-immobilized bioreporter could successfully detect formaldehyde in both solution and the gas phase at concentrations minimum of 7.5 $\mu\text{g/mL}$ and 8.1 ppm, respectively. These detection limits are useful for monitoring cumulative doses of bioavailable formaldehyde and taking precaution to avoid acute toxicity of formaldehyde. This bioreporter system is simple, low-cost, performable at room temperature and free of sample pre-treatment. The findings of this study will facilitate future research for the creation of portable and user-friendly devices for on-site and real-time environmental formaldehyde detection.

Keywords: Formaldehyde, bio-sensing, bacterial bioreporter, green fluorescent protein, alginate bead

54

55 **1. Introduction**

56 Formaldehyde (FA) is a flammable, colorless aldehyde compound (molecular formula CH_2O)
57 with a pungent unpleasant odor. Gaseous formaldehyde is one of the most toxic volatile organic
58 compounds (VOCs) and regarded as a ubiquitous air pollutant. Formaldehyde has a high
59 aqueous solubility, and the commercial form of FA is known as formalin which is an aqueous
60 solution consisting of 30-50 % FA by weight [1,2]. Formaldehyde is a widespread chemical
61 pollutant in air, water and soil because it is broadly produced and used in various industrial
62 fields. It is used as antimicrobial and preservative agent in food industry, in the manufacturing
63 of synthetic resins, binders, adhesives, plastics, paints, surface coatings, wood-based products
64 (e.g., furniture, panels, particle board and plywood), flooring and building materials, as a
65 coupling agent for textile finishing, and as a disinfectant and fixative in laboratories, mortuaries
66 and in many consumers health and cleaning products. It is also released into the ambient air as
67 a by-product in the combustion of organic compounds, on-site industrial and power plant
68 emissions, forest or bush fires, automobile exhaust and tobacco smoke [3-6].

69 As one of the most hazardous substance, many organizations have set guideline levels
70 for airborne formaldehyde. According to World Health Organization (WHO), short-term (30-
71 minute) guideline of 0.1 mg/m^3 (0.08 ppm) is recommended as safety threshold limit of
72 exposure for preventing significant sensory irritation in the general population and cytotoxic
73 damage to the nasal mucosa [1]. The Occupational Safety and Health Administration (OSHA)
74 has established the permissible exposure limit of formaldehyde in the workplace as an average
75 of 0.92 mg/m^3 (0.75 ppm) for an 8-h workday, and also the maximum short-term exposure limit
76 as 2.5 mg/m^3 (2 ppm) for 15-min period [7].

77 Gaseous formaldehyde is classified by International Agency for Research on Cancer
78 (IARC) as carcinogenic to humans (Group 1) based on the sufficient evidence in humans for
79 the nasopharyngeal cancer and leukaemia [3]. The major route of formaldehyde exposure is

80 inhalation. Acute or subsequent exposure is highly irritating to the eyes, nose, throat, and cause
81 severe allergic reactions, lachrymation, sneezing, coughing, nausea, dyspnoea since FA is a
82 highly reactive chemical and water-soluble that readily reacts with biological tissues,
83 particularly the moist mucous tissues lining the respiratory tract and the eyes [8,9]. Chronic
84 exposure to low-level formaldehyde causes respiratory diseases and allergic dermatitis which
85 is also called sick building syndrome (SBS) as a result of outgassing from household materials
86 and resins in furnitures, wallpapers or paints [10,11]. Moreover, chronic exposure of
87 formaldehyde causes neurotoxicity, inflammatory and hyperplastic changes of the nasal
88 mucosa, epithelial dysplasia, pulmonary damage, hematotoxicity, reproductive toxicity, and
89 carcinogenicity. Formaldehyde exerts its genotoxic effects by reacting with DNA, RNA and
90 protein to form adducts and cross-links such as DNA mono-adducts, DNA–DNA crosslinks,
91 DNA–protein crosslinks (DPX) and DNA glutathione cross-link resulting in DNA strand
92 breaks, chromosomal aberration, micronucleus formation and sister chromatid exchange
93 [1,3,8,12,13].

94 As the knowledge and awareness of the harmful effects of formaldehyde become more
95 obvious, the air quality and monitoring of the ambient and indoor air appear to be important
96 issues to reduce the risk of damaging health effects of gaseous formaldehyde [14,15]. The most
97 widely used traditional methods for the determination of the concentration of formaldehyde in
98 air are based on spectrophotometry, with which sensitivities of 0.01–0.03 mg/m³ can be
99 achieved. Other analytical methods involve colorimetry, fluorimetry, high-performance liquid
100 chromatography (HPLC), gas chromatography (GC), capillary electrophoresis, polarography,
101 conductometry, infrared detection and gas detector tubes [4,16-18]. These methods show
102 certain limitations such as the need of expensive and bulky instrumentation and well-trained
103 operators, operational complexity, non-portability, inutility in real-time or routine monitoring
104 and finally lack of toxicity detection. Thus, the development of sensitive, selective and facile

105 methods for fast and cost-effective FA detection for rapid estimation of personal exposure is
106 still a hot research topic [4,6,15,19].

107 Various sensor-based approaches or combinations of different methods have been
108 investigated for practical analysis of formaldehyde such as fluorescent probes [20], metal oxide
109 films and semiconductors [21,22], piezoelectricity [23], quartz crystal microbalance [24,25],
110 chemoresistive gas sensors [26], electrochemical [27,28], enzyme-based [29,30], and molecular
111 imprinting [31,32]. The use of whole cell biosensors (WCBs) is another promising approach
112 for detection of air pollutants. Unlike the aforementioned air monitoring technologies, WCBs
113 (genetically engineered living cells) are able to assess the toxicity and bioavailability of the
114 pollutant of interest [33,34].

115 Ever since the development of bacterial genotoxicity assay, the Ames test in 1973, in
116 which strains of *Salmonella typhimurium* were used as mutagenicity or genotoxicity reporters
117 [35], numerous and diverse genetically engineered bacterial bioreporters have been produced
118 for environmental monitoring of specific or group of toxic pollutants in water, soil and air [36-
119 39]. The basic principle of bacterial bioreporter is the combination of promoter-operator DNA
120 region which acts as a pollutant sensing element and a downstream reporter DNA element
121 which is translated into a detectable signal protein by using an appropriate bacterial host strain
122 having a suitable genetic background allowing movement of the pollutant across the cell,
123 recognition of the specific promoter and insignificant reporter background activity [40,41].

124 Since formaldehyde is a genotoxic chemical, one of the strategies of bioreporter
125 construction for FA detection is to employ the DNA damage-inducible promoter of *recA* gene
126 which produces the key regulatory protein of the well-defined bacterial SOS DNA repair
127 system. The bacterial SOS regulon has more than 40 unlinked genes for DNA damage tolerance
128 and error-prone replication (e.g., *dnaQ*, *uvrA*, *uvrB*, *recA*, *recN*, *sulA*, *umuC*, *umuD*) which are
129 expressed in the cell at a basal level and controlled by the LexA transcriptional repressor protein

130 which binds SOS box (LexA-binding sites) of these inducible genes at various strengths. After
131 bacterial cells are exposed to DNA damaging agents such as UV-irradiation or mutagens, the
132 RecA proteins become activated by single-stranded DNA formation and catalyzes the self-
133 cleavage of LexA protein thus allowing the high-level expression of SOS regulon genes
134 including *recA* itself to repair the damaged DNA. Thus, RecA protein has an important role for
135 initiation of the SOS response and has a broad involvement in many DNA repair pathways,
136 including daughter-strand gaps, double-strand breaks, and error prone DNA damage survival
137 mechanisms [42-44].

138 The aim of this study is to develop a bacterial bioreporter system for gaseous
139 formaldehyde detection. A fluorescent bioreporter strain, *Escherichia coli* (pBR-PrecA),
140 harboring a plasmid-borne transcriptional fusion between the *E. coli recA* gene promoter and
141 *gfpuv* (green fluorescent protein) reporter gene was constructed. Thus, formaldehyde will
142 induce the derepression of *recA* promoter which increase the expression of downstream GFP
143 and increase the fluorescent signals to be measured. The testing of gaseous formaldehyde has
144 been made feasible by immobilization of FA bioreporter into alginate hydrogel matrix
145 permitting semi-direct contact between the sensor bacteria and FA gas. Sodium alginate was
146 chosen as immobilization polymer since it is commonly used for cell immobilization due to its
147 easy and gentle preparation conditions, its hydrogel environment enabling cells the
148 maintenance of cell activity over a long period and providing a mechanical support and plasmid
149 stability. Moreover, immobilization enables portability and long-term measurement in contrast
150 to liquid culture [34,45]. Only limited research is available in the literature regarding gaseous
151 formaldehyde detection by using WCBs. To the best of our knowledge, this is the first study
152 for gaseous formaldehyde sensing by using alginate bead-immobilized *recA*-based fluorescent
153 *E. coli* bioreporter. The developed alginate bead-immobilized bioreporter cells are able to detect

154 formaldehyde in both liquid and gaseous phases and offer a simple and cost-effective method
155 for monitoring of toxic formaldehyde.

156 **2. Materials and methods**

157 *2.1. Bacterial strains, media and chemicals*

158 *E. coli* DH5 α strain was used for promoter cloning experiments. *E. coli* MG1655 (ATCC
159 700926) was used as host strain for bioreporter construction. LB (Luria-Bertani) broth (10 g/L
160 tryptone, 5 g/L yeast extract, 10 g/L NaCl, pH 7.0) was used for bacteria propagation. Mineral
161 salt supplemented medium (MSSM), (10 mM Na₂HPO₄, 5 mM KH₂PO₄, 34.2 mM NaCl, 12.5
162 mM NH₄NO₃, 2 mM MgSO₄, 0.2 mM CaCl₂, 35 μ M FeCl₃, 0.1 % (w/v) casamino acids, 0.5 %
163 (w/v) glucose, pH 7.0) was used as an induction and immobilization medium. Ampicillin (100
164 μ g/mL) was used for plasmid maintenance. Formaldehyde solution (formaline), 37% technical
165 grade (Applichem A2628) was used as the inducer. Formaldehyde (MW: 30.03 g/mol)
166 concentration of formalin is 12.3 M. Alginate acid sodium salt (Sigma-Aldrich 71238) was used
167 for alginate bead immobilization experiments.

168 *2.2. Construction of the sensor plasmid*

169 The formaldehyde sensing DNA sequence belonging to the promoter region of the *recA* gene
170 (NCBI Gene ID: 947170) were obtained from *E. coli* MG1655 genome (GenBank Accession
171 Number U00096.3). *E. coli* MG1655 genomic DNA was isolated by using Nanobiz DNA4U
172 Bacterial Genomic DNA Isolation Kit (Turkey) for gram-negative bacteria and used as the
173 template for amplification of the promoter region. The high-fidelity polymerase chain reaction
174 (Hi-Fi PCR) of *recA* promoter was done by using Phusion DNA polymerase (Thermo Scientific,
175 USA) using forward primer recAp-F (5'GTGACAGAATTCGTCACCTACAGTAACGAA
176 GCC3') and reverse primer recAp-R (5'GTATGTGGATCCTACTCCTGTCATGCCGGG'3).
177 The amplified 427 base-pair DNA fragment was then digested with the *EcoRI* and *BamHI*
178 restriction enzymes and then inserted at the same restriction sites into formerly constructed

179 promoterless reporter plasmid ‘pBR-sGFP’ [46]. The final construct was confirmed using
180 agarose gel electrophoresis and Sanger sequencing using the oligonucleotides which are
181 forward primer Col-F (5’ATCACGAGGCCCTTTCGTCTTCAAGAATTC3’) and reverse
182 primer Col-R (5’ACGCTGCCCGAGTTATCATTATTTGTAGAGCTC3’). The resulting
183 sensor plasmid designated as ‘pBR-PrecA’ was chemically transformed into chemically
184 competent *E. coli* MG1655 cells. The plasmid map was generated using Snapgene software
185 (GSL Biotech, USA).

186 *2.3. Induction of free bioreporter cells with liquid formaldehyde*

187 The overnight-grown bioreporter cells were inoculated into 10 mL of mineral salt supplemented
188 medium (MSSM) at a 1:20 (v/v) ratio in 50 mL conical tubes. Diluted aqueous solutions of
189 formaline was added to bacterial cultures at final formaldehyde concentrations of 50, 100, 250,
190 500, 750 and 1000 μ M (1.5, 3, 7.5, 15, 22.5 and 30 μ g/mL) including a negative control (sterile
191 distilled water). The tubes were incubated at 35 °C on a shaker at 180 rpm for 24 hours. The
192 cell growth was monitored via measuring optical density at 600 nm by using Multiskan GO
193 UV/Visible Microplate and Cuvette Spectrophotometer (Thermo Fisher Scientific, USA). The
194 fluorescence measurements were done by applying 200 μ L of each culture into 96-well standard
195 black microplates (Greiner Bio-One) at different time points by using SpectraMax iD3
196 (Molecular Devices, USA) multi-mode microplate reader. The fluorescence measurements
197 were taken at excitation and emission wavelengths of 395 and 509 nm, respectively, for the
198 reporter green fluorescent protein, GFPuv [47]. Induced cells were observed using an EVOS
199 Fluid Imaging Station (Thermo Fisher Scientific, USA) under illumination of blue channel with
200 excitation 390 ± 40 nm and emission 446 ± 33 nm.

201 *2.4. Immobilization of bioreporter cells into alginate beads*

202 Aqueous solutions of alginic acid sodium salt of 2% (w/v) were prepared one day before making
203 beads for polymer stabilization. Overnight bioreporter bacterial culture was subcultured in

204 MSSM and exponentially grown bacteria were centrifuged at 3500 xg and 15 °C for 8 mins.
205 Cell pellets were gently re-suspended in fresh MSSM to optical density at 600 nm (OD₆₀₀) of
206 0.4 (1 unit of OD₆₀₀ = 8×10⁸ cells/mL). The prepared bioreporter bacterial culture was
207 homogeneously mixed with alginate solution in a 1:1 (v/v) ratio and gently stirred for 15 mins.
208 The mixture was dripped from a 10 mL syringe with a 2 mm inner diameter spout that was
209 mounted on a syringe pump into a 0.3 M CaCl₂ solution in a glass beaker with magnetic stirrer
210 at a flow rate of 100 μL/sec. 1 mL of alginate-cell mixture generated an average of 30 beads
211 [48]. The beads that spontaneously formed were stirred for additional 30 mins to ensure a
212 complete gelation process. After rinsing with sterile distilled water to remove excess calcium
213 chloride and untrapped cells, the alginate beads were damp-dried on filter paper and stored
214 at 4 °C until use.

215 *2.5. Liquid formaldehyde detection by immobilized bioreporter cells*

216 Thirty beads were placed in 50 mL conical tubes and 4 mL of 1:2 (v/v) diluted aqueous MSSM
217 solution (0.5X MSSM) was added. Serial dilutions of aqueous formaldehyde solutions having
218 final concentrations of 50, 100, 250, 500, 750 and 1000 μM including a negative control (sterile
219 distilled water) were prepared on a daily basis. The tubes were incubated at 35 °C with gentle
220 agitation for 16 hours. Fluorescence measurements were performed by placing three beads in
221 the wells of 96-well microplate and data obtained by using SpectraMax iD3 multi-mode
222 microplate reader at different time points at excitation/emission wavelength of 395/509 nm.

223 *2.6. Gaseous formaldehyde detection by immobilized bioreporter cells*

224 Between 25 and 30 alginate-cell beads were transferred to small plastic Petri dishes (40 mL in
225 volume) and 3 mL of different assay solutions were added to beads in order to prevent
226 desiccation and shrinkage of alginate hydrogel beads. These Petri dishes were placed into 5-L
227 plastic storage boxes. Then, 20 mL of aqueous dilutions of formalin solutions having
228 concentrations of 300 mM, 150 mM, 100 mM, 60 mM and 30 mM (FA concentrations of

229 including a negative control (distilled water) in a glass beaker were placed at the center of the
230 storage boxes. Then the boxes were closed tightly and incubated under controlled temperature
231 at 25 °C for 16 hours at 60 rpm shaking. Formaldehyde gas concentrations generated from the
232 liquid-vapor equilibrium of diluted formalin solutions at 25 °C were determined by using
233 Henry's law formula below [4,49] and using a $H_{eff} = 3700 \text{ M atm}^{-1}$.

$$234 \quad P(atm) = \frac{\text{Concentration (M)}}{H_{eff}(\text{M} \cdot \text{atm}^{-1})}$$

$$235 \quad ppm = P(atm) \cdot 10^6$$

236 By applying these formula, FA gas concentrations (after saturation) in the boxes were calculated
237 as 81, 40.5, 27, 16.2 and 8.1 ppm, respectively. At determined time points, three beads were
238 quickly taken from the Petri dish without disturbing the system and placed into 96-well black
239 microplate and fluorescence measurements were taken immediately as described above.

240 *2.7. Testing different bead assay solutions*

241 For vapor phase experiments, tested bead assay solutions include sterile deionized water,
242 mineral salt supplemented medium (1X MSSM), 1:2 and 1:4 (v/v) diluted aqueous MSSM
243 solutions (0.5X MSSM and 0.25X MSSM), 0.2 mM CaCl_2 solution, and 1X PBS (phosphate-
244 buffered saline).

245 *2.8. Gas specificity of immobilized bioreporter cells*

246 For gas specificity test, some of common volatile toxic solutions were tested. 100 mM of
247 aqueous solutions of glacial acetic acid, acetone, chloroform, isopropanol, methanol, and
248 xylenes were prepared including negative control and 20 mL of each solution was placed in
249 their respective boxes. Then the boxes were closed tightly and incubated at controlled
250 temperature at 25 °C. At the end of 16 hours, three beads were placed into 96-well black
251 microplate and then fluorescence measurements were taken immediately as described above.

252 *2.9. Data analysis*

253 All statistical analyses were conducted using the IBM SPSS Statistics 25.0 software package
254 for Windows. The response of bioreporter cells was indicated by fluorescence intensity. Raw
255 fluorescence intensities were expressed in the instrument's arbitrary relative fluorescence units
256 (RFU). The (normalized) fluorescence response was calculated by subtracting induced culture
257 fluorescence from background *E. coli* MG1655 (pBR-sGFP) (promoterless bioreporter) culture
258 fluorescence for all concentrations at the corresponding time points. All tests were performed
259 in triplicate and results were expressed as mean values with standard deviations which were
260 represented by error bars in the graphs. The limit of detection or the detection limit was set at
261 the lowest concentration of formaldehyde that is detected under the stated experimental
262 conditions. The one-way analysis of variance (one-way ANOVA) was performed with the
263 significance level of 0.05 ($p < 0.05$) followed by Tukey's post hoc comparison test between
264 RFU values of induced and uninduced samples to determine the detection limits.

265 **3. Results and discussion**

266 *3.1. Bioreporter strain construction*

267 For the development of whole cell bacterial bioreporter for formaldehyde detection, a sensor
268 plasmid, designated as pBR-PrecA, (Fig 1) containing promoterless green fluorescent protein
269 gene (*gfpuv*) under the control of *recA* gene promoter, was constructed and then transformed to
270 *E. coli* MG1655 host strain. As being one of the key SOS response genes that is responsible for
271 error-prone DNA repair to survive sudden or extensive DNA damage [50], the application of
272 the *recA* promoter is useful for development of efficient bacterial biosensors for genotoxic
273 formaldehyde detection. Upon FA exposure, RecA proteins became activated in the cells
274 causing derepression of *recA* promoters by the release the LexA repressor protein and the
275 expression of reporter *gfpuv* was induced. The developed FA bioreporter, *E. coli* (pBR-PrecA),
276 was tested against liquid and gaseous formaldehyde, and the bioreporter response was obtained
277 by measuring green fluorescent protein (GFPuv) signals.

278 3.2. Induction of free bioreporter cells with liquid formaldehyde

279 In order to confirm the applicability of FA bioreporter cells, the liquid FA induction tests were
280 done with FA concentrations between 50 and 1000 μM . Firstly, the growth of the bioreporter
281 cells was monitored to assess the toxicity of formaldehyde on bacterial cells (Fig 2a). Bacterial
282 cells tolerated liquid formaldehyde concentrations of up to 750 μM (22.5 $\mu\text{g}/\text{mL}$) and 1 mM
283 FA (30 $\mu\text{g}/\text{mL}$) was found toxic at which no cell growth was observed.

284 Ptitsyn et al. [51] constructed a genotoxin bioreporter by fusing *cda* promoter upstream
285 of the promoterless *luxCDABFE* genes and they also reported a small dynamic range of
286 detection which is between 0.3 and 0.75 mM that formaldehyde concentration higher than 750
287 μM was highly cytotoxic and no light emission could be detected, similar to the present
288 findings.

289 Fig 2b shows the time- and dose-dependent fluorescence response of the bioreporter to
290 liquid FA presented during 16-h induction period. The detection limit was determined using
291 statistically significant changes ($p < 0.05$) in RFU compared with no induction control RFU.
292 One-way ANOVA results showed that the FA bioreporter induction was significant after 4
293 hours ($p = 0.00$) by all the tested concentrations of formaldehyde except 1 mM of FA which was
294 very toxic and inhibited the cell growth. However, after 8 hours due to increased background
295 fluorescence only 250, 500 and 750 μM showed a fluorescence response with a statistically
296 significant change ($p < 0.05$). The prominent response was obtained from 15 $\mu\text{g}/\text{mL}$ (500 μM)
297 of FA at 4-h and 8-h time points and 22.5 $\mu\text{g}/\text{mL}$ (750 μM) FA induction continued to increase
298 after 8 hours contrast to other concentrations which tend to decline after 8 hours.

299 According to World Health Organization [52] formaldehyde is not carcinogenic by the
300 oral route and they did not set a guideline value in drinking water stating that the occurrence of
301 formaldehyde is below the concentrations of health concern. However, US EPA has advised
302 that the exposure to formaldehyde in drinking water health advisory limit of 10 mg/L for 1 day

303 or 5 mg/L for 10 days for 10 kg child. Moreover, The US EPA has also determined that a
304 lifetime exposure to 1 mg/L of formaldehyde in drinking water is not expected to cause any
305 adverse health effects [53]. Thus, since the developed FA bioreporter has detection range
306 between 1.5 and 22.5 mg/L, it can be used detect these advised exposure limits.

307 Bacterial bioreporters constructed by the fusion of the *recA* promoter to a reporter gene
308 has been regarded as an effective genotoxicity sensor for genotoxic agents as mitomycin C
309 (MMC), nalidixic acid (NA), methylnitronitrosoguanidine (MNNG), dimethylsulfate,
310 hydrogen peroxide (H₂O₂), bisphenol A, etc. and developed over the last two decades [54-60].
311 Formaldehyde has been also detected by *recA*-based bacterial genotoxicity bioreporters [61-
312 65].

313 Kostrzynska et al. [62] constructed *E. coli* C600 cells carrying pRGW50 or pRGM5
314 plasmids based on *recA* promoter fused to wild type *gfp* or red-shifted variant *gfp* (mut3) to
315 perform genotoxicity test. Besides nalidixic acid, MMC, MNNG, hydrogen peroxide they also
316 tested formaldehyde. They report the detection limit for FA 305±51 µM and small dynamic
317 range (200-800 µM) for *recA* induction. They also indicated that higher concentrations
318 significantly diminished viability of cells. Kuang et al. [63] employed *E. coli*
319 MG1655+pUA2699 carrying a *recA::gfp* fusion plasmid. They performed microtiter assay in
320 M9 medium and tested 10 µg/mL of MMC, MNNG, H₂O₂, FA and NA. They reported much
321 weaker fluorescence response from FA compared to MMC and reported that cells induced with
322 FA concentrations of 0.1 mg/mL (3.3 M) had high fluorescence response with no lethal effect.
323 Matejczyk [64] used *E. coli* K-12 MG1655 (pUA66) strain having *recA* promoter fused with
324 *gfp* mutated gene – GFPmut2 variant. The tested concentrations of FA were between 50 and
325 1800 mg/ml which was too high compared to the present study. It was reported that 900 mg/mL
326 (30 M) FA was found to induce highest fluorescence.

327 Fig 2c compares the uninduced bioreporter cells and induced cells with 500 μM
328 formaldehyde (15 $\mu\text{g/mL}$). While uninduced cells had no visible emission, induced cells
329 showed a bright fluorescence emission, and some of the FA exposed cells were seen as very
330 long cells. The explanation for this phenomenon can be that as genotoxic FA causes cell
331 replication to stall, RecA proteins are recruited to DNA at the stalled replication forks then
332 activating Sula-mediated cell division inhibition. This leads to cell filamentation and increase
333 in the ratio of elongated cells due to inhibition of cell division for the fast-growing *E. coli* cells
334 [66,67].

335 *3.3. Immobilization of bioreporter cells into alginate beads*

336 Since the developed FA bioreporter was found to be applicable in formaldehyde detection
337 according to the results of liquid culture broth induction, the bacterial bioreporter cells were
338 entrapped in a suitable immobilization matrix for convenient gas detection. Immobilization
339 enables portability, on-site detection ability and integration into mobile devices. By bioreporter
340 immobilization, direct testing of the gaseous FA has been made possible in a way that liquid
341 FA evaporated during incubation time and then diffused through the air directly to the entrapped
342 bacteria [68,69].

343 Ca-alginate beads are widely used hydrogel matrices in which cells are passively and
344 non-covalently entrapped into the gel matrix under mild physicochemical conditions.
345 Moreover, alginate hydrogel beads have high porosity due to their open lattice structure and
346 confer gentle environment that makes them an optimal choice for cell entrapment also enabling
347 analyte diffusion and metabolite secretion. As described in Fig 3, the beads were produced by
348 mixing bioreporter culture and sodium alginate solution and by extruding this mixture dropwise
349 into calcium chloride solution where Ca-alginate beads are formed spontaneously by rapid
350 crosslinking between negatively charged alginate polymers and positively charged divalent
351 calcium ions [70,71]. The alginate immobilization optimized parameters in terms of final

352 alginate concentration of 1% (w/v) and bacterial cell density in the matrix of OD₆₀₀ 0.25 [48]
353 were employed in this study.

354 3.4. Liquid formaldehyde detection by immobilized cells

355 Prior to testing with gaseous formaldehyde, bead immobilized FA bioreporter was tested
356 against liquid formaldehyde (aqueous dilutions of formalin). FA concentrations between 50 and
357 1000 μM were tested to obtain time- and dose-dependent fluorescence responses.

358 The fastest and highest fluorescence response was obtained with 500 μM (15 μg/mL) of
359 FA within a 4 h-induction (Fig 4a). The lowest detection limit of liquid FA was obtained at 250
360 μM (7.5 μg/mL) within 8 hours and the highest FA concentration of 750 μM (22.5 μg/mL) was
361 detected after 8 hours with a statistically significant change (p<0.05). As with the case of free
362 cells, 1 mM FA showed lowered fluorescence compared to that of control with no FA treatment
363 indicating its lethal effects. Fig 4b shows the comparison between the uninduced bioreporter
364 beads (control) and induced beads with 500 μM formaldehyde (15 μg/mL). While for
365 uninduced cells only excitation wavelength (blue) was visible, induced cells displayed a marked
366 green emission due to GFP fluorescence.

367 There are few studies for immobilized *recA*-based bioreporter systems for liquid
368 formaldehyde detection. Eltzov et al. [72] immobilized *E. coli* DPD2794 strain having plasmid-
369 borne fusion of the *recA* promoter to a *luxCDABE* reporter operon into calcium alginate pads
370 coupled to photodetector. They tested this strain against various chemicals including liquid
371 formaldehyde between 10⁻⁶ and 10⁻¹⁴ M and the strain was not sensitive against formaldehyde
372 which is probably due to very low tested concentrations.

373 3.5. Gaseous formaldehyde detection by immobilized cells

374 For gaseous FA induction, the experimental setup in Fig 5 was used. Firstly, the beads were
375 placed in Petri dishes without a lid and assay solutions were added on them. The Petri dishes
376 were then put in a 5-L storage boxes. The serial dilutions of formalin solutions and water

377 (negative control) were placed at the center of the boxes. Finally, the boxes were closed tightly
378 and placed on orbital shakers for better evaporation of solutions and aeration of beads.
379 Formaldehyde in the aqueous solutions was considered to evaporate completely during the
380 experiment time and expected to diffuse into alginate beads to induce GFP expression in
381 bioreporter bacteria.

382 *3.6. Testing different bead assay solutions*

383 Unlike the liquid induction tests, this time alginate beads were exposed to air for hours, so they
384 were highly prone to dehydration and shrinkage. These hydrogel beads should be kept moist
385 during induction to avoid loss of water, to sustain cell viability and bioreporter activity inside
386 the beads. For these reasons, assay (preservation) solutions were added on the beads in a small
387 amount to keep them hydrated. Different solutions were tested to find the most suitable assay
388 solution presenting higher fluorescence performance and sensitivity.

389 As seen in Fig 6, MSSM and 0.5X (1/2 strength) MSSM provided the highest
390 fluorescence responses whereas 0.25X MSSM had comparably low RFU values. The other
391 solutions such as, water, calcium chloride and 1X PBS did not produce any response probably
392 due to the fact that they could not support the metabolic activity of the cells to recover from the
393 toxic effects of FA or to express sufficient amount of reporter protein. It should be noted that
394 the main disadvantage of using alginate-based hydrogels is its tendency to dissolve in presence
395 of low pH, high concentrations of non-gelling ions (e.g., Na⁺, Mg²⁺, and K⁺), polyphosphates,
396 citric acid and EDTA solutions [73]. Therefore, the composition of assay solution should be
397 optimized to keep the integrity of hydrogel beads to withstand hours and to avoid releasing of
398 immobilized cells. This case was observed with the tested 1X PBS assay solution which has a
399 high sodium and potassium content.

400 *3.7. Dose-dependent response of beads to different formaldehyde vapor concentrations*

401 After determining the most suitable assay solutions that are MSSM and 0.5X MSSM, the
402 immobilized bioreporter was tested in these assay solutions at different FA gas concentrations.

403 For MSSM assay solution, according to one-way ANOVA results, the induction of
404 bioreporter was significant within 8 hours ($p=0.00$) and the detection limit was 8.1 ppm of gas
405 FA. For 16-h incubation, gaseous FA at 27 and 40.5 ppm exhibited increased fluorescence (Fig
406 7a) which could be attributed to that these gaseous formaldehyde level in the box kept the cells
407 stressed for a longer time, when compared to lower FA levels. When 0.5X MSSM assay
408 solution was used, the sensitivity of bioreporter decreased to 16.2 ppm after 8 hours and the
409 fluorescence responses were somewhat lower compared to that of MSSM for all data points
410 (Fig 7b) which can be due to lower nutrient content of half-strength MSSM solution. For both
411 assay solutions, gaseous formaldehyde of 81 ppm did not produce significant fluorescence
412 response due to possible toxicity to immobilized cells.

413 *3.8. Gas specificity of immobilized bioreporter cells*

414 For assessment of gas specificity or selectivity of the FA bioreporter, aqueous solutions of
415 commonly used volatile compounds, acetic acid, acetone, chloroform, isopropanol, methanol,
416 and xylenes were tested.

417 As shown in Fig 8, for both MSSM and 0.5X MSSM assay solutions, among tested
418 volatile compounds, acetone which is also an aldehyde, and methanol induced the bioreporter,
419 but the fluorescence responses were less than half of those induced by formaldehyde. Upon
420 most occurrences both outdoor and indoor, formaldehyde gas is the predominant form of
421 environmental aldehydes [74], and the developed FA bioreporter showed a significantly higher
422 selectivity for formaldehyde.

423 **4. Conclusion**

424 This study presents the development of an alginate-immobilized fluorescent bacterial
425 bioreporter for both liquid and gaseous formaldehyde detection. The bioreporter cells entrapped

426 in alginate beads are able to detect liquid formaldehyde concentrations as low as 7.5 µg/mL
427 within 4 hours and are able to indicate biologically harmful levels of formaldehyde. To our
428 best knowledge, no studies have been conducted for immobilized *recA*-based bioreporter
429 systems characterized for gaseous formaldehyde detection. The bioreporter described could
430 detect gaseous formaldehyde levels as low as 8.1 ppm in air. Even though it has high gas
431 detection limits compared to standard analytic methods, it is capable of detecting cumulative
432 doses over 8 hours which can be considered similar to an 8-h working day. Moreover, it has a
433 good specificity for formaldehyde and its detection limit can be improved by using more
434 sensitive detection methods such as using very bright fluorescent proteins [75] or tandem
435 fluorescent protein constructs [76]. The reported bioreporter system is simple, cost-effective,
436 operates at room temperature and requires no sample preparation. It can be further developed
437 to be used in handheld environmental monitoring kits or in remote-controlled sensor devices
438 for on-site formaldehyde monitoring.

439 **Funding**

440 This work was supported by The Scientific and Technical Research Council of Turkey 2522
441 TUBITAK (Turkey)-NRDIO (Hungary) Joint Funding Program (Project No: 217E115);
442 NRDIO-NKFIH (Grant No: 129987); and Nanobiz Technology Inc.

443 **References**

- 444 [1] D.A. Kaden, C. Mandin, G.D. Nielsen, P. Wolkoff, Formaldehyde, in: WHO Guidelines for
445 Indoor Air Quality: Selected Pollutants, World Health Organization, Geneva, 2010. 3. pp
446 103-156.
- 447 [2] World Health Organization (WHO), Formaldehyde, in: Air quality guidelines for Europe,
448 2nd edition, WHO Regional Publications, European Series, No. 91, Copenhagen, 2000, pp.
449 87-91.

- 450 [3] International Agency for Research on Cancer (IARC), Formaldehyde, in: IARC
451 Monographs on the evaluation of carcinogenic risks to humans, Volume 100F, Lyon,
452 France, 2012, pp. 401-435.
- 453 [4] C. Martínez-Aquino, A.M. Costero, S. Gil, P. Gaviña, A new environmentally-friendly
454 colorimetric probe for formaldehyde gas detection under real conditions, *Molecules*. 23 (10)
455 (2018) 2646. <https://doi.org/10.3390/molecules23102646>.
- 456 [5] T. Salthammer, S. Mentese, R. Marutzky, Formaldehyde in the indoor environment, *Chem.*
457 *Rev.* 110 (2010) 2536–2572. <https://doi.org/10.1021/cr800399g>.
- 458 [6] S. Sigawi, O. Smutok, O. Demkiv, G. Gayda, B. Vus, Y. Nitzan, M. Gonchar, M.
459 Nisnevitch, Detection of waterborne and airborne formaldehyde: from amperometric
460 chemosensing to a visual biosensor based on alcohol oxidase, 7 (2014) 1055–1068.
461 <https://doi.org/10.3390/ma7021055>.
- 462 [7] Occupational Safety and Health Administration (OSHA). Occupational Safety and Health
463 Standards, Toxic and hazardous substances, Code of Federal Regulations 29 CFR
464 1910.1048, 2007.
- 465 [8] K.H. Kim, S.A. Jahan, J.T. Lee, Exposure to formaldehyde and its potential human health
466 Hazards, *J. Environ. Sci. Heal. - Part C Environ. Carcinog. Ecotoxicol. Rev.* 29 (4) (2011)
467 277–299. <https://doi.org/10.1080/10590501.2011.629972>.
- 468 [9] G.D. Nielsen, S.T. Larsen, P. Wolkoff, Re-evaluation of the WHO (2010) formaldehyde
469 indoor air quality guideline for cancer risk assessment, *Arch. Toxicol.* 91 (2017) 35–61.
470 <https://doi.org/10.1007/s00204-016-1733-8>.
- 471 [10] K. Kawamura, K. Kerman, M. Fujihara, N. Nagatani, T. Hashiba, E. Tamiya,
472 Development of a novel hand-held formaldehyde gas sensor for the rapid detection of sick
473 building syndrome, *Sens. Actuators B Chem.* 105 (2005) 495–501.
474 <https://doi.org/10.1016/j.snb.2004.07.010>.

- 475 [11] M. Takeda, Y. Saijo, M. Yuasa, A. Kanazawa, A. Araki, R. Kishi, Relationship between
476 sick building syndrome and indoor environmental factors in newly built Japanese dwellings,
477 *Int. Arch. Occup. Environ. Health.* 82 (2009) 583–593. [https://doi.org/10.1007/s00420-009-](https://doi.org/10.1007/s00420-009-0395-8)
478 0395-8.
- 479 [12] M. Kawanishi, T. Matsuda, T. Yagi, Genotoxicity of formaldehyde: molecular basis of
480 DNA damage and mutation, *Front. Environ. Sci.* 2 (2014) 1–8.
481 <https://doi.org/10.3389/fenvs.2014.00036>.
- 482 [13] National Research Council, Review of the Environmental Protection Agency's Draft
483 IRIS Assessment of Formaldehyde, The National Academies Press. Washington, DC, 2011.
- 484 [14] E. Eltzov, A.L. De Cesarea, Y.K.A. Low, R.S. Marks, Indoor air pollution and the
485 contribution of biosensors, *EuroBiotech J.* 3 (2019) 19–31. [https://doi.org/10.2478/ebtj-](https://doi.org/10.2478/ebtj-2019-0003)
486 2019-0003.
- 487 [15] D. Kukkar, K. Vellingiri, R. Kaur, S.K. Bhardwaj, A. Deep, K. Kim, Nanomaterials for
488 sensing of formaldehyde in air: principles, applications, and performance evaluation, 12 (2)
489 (2019) 225–246. <https://doi.org/10.1007/s12274-018-2207-5>.
- 490 [16] O. Bunkoed, F. Davis, P. Kanatharana, P. Thavarungkul, S.P.J. Higson, Sol-gel based
491 sensor for selective formaldehyde determination, *Anal. Chim. Acta.* 659 (2010) 251–257.
492 <https://doi.org/10.1016/j.aca.2009.11.034>.
- 493 [17] P.-R. Chung, C.-T. Tzeng, M.-T. Ke, C.-Y. Lee, Formaldehyde gas sensors: a review,
494 *Sensors* 13 (2013) 4468–4484. <https://doi.org/10.3390/s130404468>.
- 495 [18] International Agency for Research on Cancer (IARC), Formaldehyde, 2-butoxyethanol
496 and 1-tertbutoxypropan-2-ol, in: IARC Monographs on the evaluation of carcinogenic risks
497 to humans, Lyon, France, 2006, 88, pp. 39-325.

- 498 [19] X.-L. Guo, Y. Chen, H.-L. Jiang, X.-B. Qiu, D.-L. Yu, Smartphone-based microfluidic
499 colorimetric sensor for gaseous formaldehyde determination with high sensitivity and
500 selectivity, *Sensors* 18 (2018) 3141. <https://doi.org/10.3390/s18093141>.
- 501 [20] X. Liu, N. Li, M. Li, H. Chen, N. Zhang, Y. Wang, K. Zheng, Recent progress in
502 fluorescent probes for detection of carbonyl species: formaldehyde, carbon monoxide and
503 phosgene, *Coord. Chem. Rev.* 404 (2020) 213109.
504 <https://doi.org/10.1016/j.ccr.2019.213109>.
- 505 [21] J. Flueckiger, F.K. Ko, K.C. Cheung, Microfabricated formaldehyde gas sensors,
506 *Sensors* 9 (2009) 9196–9215. <https://doi.org/10.3390/s91109196>.
- 507 [22] Z. Han, Y. Qi, Z. Yang, H. Han, Y. Jiang, W. Du, X. Zhang, J. Zhang, Z. Dai, L. Wu,
508 C. Fletcher, Z. Wang, J. Liu, G. Lu, F. Wang, Recent advances and perspectives on
509 constructing metal oxide semiconductor gas sensing materials for efficient formaldehyde
510 detection, *J. Mater. Chem. C* 8 (2020) 13169–13188. <https://doi.org/10.1039/d0tc03750h>.
- 511 [23] J. Ma, S. Wang, D. Chen, W. Wang, Z. Zhang, S. Song, W. Yu, ZnO piezoelectric film
512 resonator modified with multi-walled carbon nanotubes/polyethyleneimine bilayer for the
513 detection of trace formaldehyde, *Appl. Phys. A Mater. Sci. Process.* 124 (2018).
514 <https://doi.org/10.1007/s00339-017-1481-5>.
- 515 [24] L. Wang, J. Gao, J. Xu, QCM formaldehyde sensing materials: design and sensing
516 mechanism, *Sens. Actuators B Chem.* 293 (2019) 71–82.
517 <https://doi.org/10.1016/j.snb.2019.04.050>.
- 518 [25] M. Yang, J. He, Graphene oxide as quartz crystal microbalance sensing layers for
519 detection of formaldehyde, *Sens. Actuators B Chem.* 228 (2016) 486–490.
520 <https://doi.org/10.1016/j.snb.2016.01.046>.

- 521 [26] J. van den Broek, D. Klein Cerrejon, S.E. Pratsinis, A.T. Güntner, Selective
522 formaldehyde detection at ppb in indoor air with a portable sensor, *J. Hazard. Mater.* 399
523 (2020) 123052. <https://doi.org/10.1016/j.jhazmat.2020.123052>.
- 524 [27] E. Menart, V. Jovanovski, S.B. Hočevár, Novel hydrazinium polyacrylate-based
525 electrochemical gas sensor for formaldehyde, *Sens. Actuators B Chem.* 238 (2017) 71–75.
526 <https://doi.org/10.1016/j.snb.2016.07.042>.
- 527 [28] D. Trivedi, J. Crosse, J. Tanti, A.J. Cass, K.E. Toghiani, The electrochemical
528 determination of formaldehyde in aqueous media using nickel modified electrodes, *Sens.*
529 *Actuators B Chem.* 270 (2018) 298–303. <https://doi.org/10.1016/j.snb.2018.05.035>.
- 530 [29] H. Kudo, Y. Suzuki, T. Gesseli, D. Takahashi, T. Arakawa, K. Mitsubayashi,
531 Biochemical gas sensor (bio-sniffer) for ultrahigh-sensitive gaseous formaldehyde
532 monitoring, *Biosens. Bioelectron.* 26 (2010) 854–858.
533 <https://doi.org/10.1016/j.bios.2010.07.099>.
- 534 [30] A. Monkawa, T. Gesseli, Y. Takimoto, N. Jo, T. Wada, N. Sanari, Highly sensitive and
535 rapid gas biosensor for formaldehyde based on an enzymatic cycling system, *Sens.*
536 *Actuators B Chem.* 210 (2015) 241–247. <https://doi.org/10.1016/j.snb.2014.11.148>.
- 537 [31] L. Feng, Y. Liu, X. Zhou, J. Hu, The fabrication and characterization of a formaldehyde
538 odor sensor using molecularly imprinted polymers, *J. Colloid Interface Sci.* 284 (2005)
539 378–382. <https://doi.org/10.1016/j.jcis.2004.10.054>.
- 540 [32] X. Tang, J.-P. Raskin, D. Lahem, A. Krumpmann, A. Decroly, M. Debliquy, A
541 formaldehyde sensor based on molecularly-imprinted polymer on a TiO₂ nanotube array,
542 *Sensors* 17 (2017) 675. <https://doi.org/10.3390/s17040675>.
- 543 [33] U. Bohrn, E. Stütz, K. Fuchs, M. Fleischer, M.J. Schöning, P. Wagner, Air quality
544 monitoring using a whole-cell based sensor system, *Procedia Eng.* 25 (2011) 1421–1424.
545 <https://doi.org/10.1016/j.proeng.2011.12.351>.

- 546 [34] N. Gupta, V. Renugopalakrishnan, D. Liepmann, R. Paulmurugan, B.D. Malhotra, Cell-
547 based biosensors: recent trends, challenges and future perspectives, *Biosens. Bioelectron.*
548 141 (2019) 111435. <https://doi.org/10.1016/j.bios.2019.111435>.
- 549 [35] B.N. Ames, F.D. Lee, W.E. Durston, An improved bacterial test system for the detection
550 and classification of mutagens and carcinogens, *Proc. Natl. Acad. Sci. USA* 70 (1973) 782–
551 786. <https://doi.org/10.1073/pnas.70.3.782>.
- 552 [36] M. Bilal, H.M.N. Iqbal, Microbial-derived biosensors for monitoring environmental
553 contaminants: recent advances and future outlook, *Process Saf. Environ. Prot.* 124 (2019)
554 8–17. <https://doi.org/10.1016/j.psep.2019.01.032>.
- 555 [37] E. Elcin, H.A. Öktem, Inorganic cadmium detection using a fluorescent whole-cell
556 bacterial bioreporter, *Anal. Lett.* 53 (17) (2020) 2715–2733.
557 <https://doi.org/10.1080/00032719.2020.1755867>.
- 558 [38] S. Jouanneau, M.J. Durand, A. Assaf, M. Bittel, G. Thouand, Bacterial bioreporter
559 applications in ecotoxicology: concepts and practical approach, in: C. Cravo-Laureau,
560 C. Cagnon, B. Lauga, R. Duran (Eds.), *Microbial Ecotoxicology*, Springer, Cham, 2017.
- 561 [39] N. Zeng, Y. Wu, W. Chen, Q. Huang, P. Cai, Whole-cell microbial bioreporter for soil
562 contaminants detection, *Front. Bioeng. Biotechnol.* 9 (2021) 1–10.
563 <https://doi.org/10.3389/fbioe.2021.622994>.
- 564 [40] A. Biran, R. Pedahzur, S. Buchinger, G. Reifferscheid, S. Belkin, Genetically
565 engineered bacteria for genotoxicity assessment, *Hdb Env Chem.* 5J (2009) 161–186.
566 <https://doi.org/10.1007/698>.
- 567 [41] M.B. Gu, R.J. Mitchell, B.C. Kim, Whole-Cell-Based Biosensors for Environmental
568 Biomonitoring and Application. *Adv Biochem Engin/Biotechnol.* 87 (2004) 269–305.
569 <https://doi.org/10.1007/b13533>.

- 570 [42] P.R. Bianco, RecA protein, in: eLS. John Wiley & Sons, Ltd, Chichester, 2019.
571 <https://doi.org/10.1002/9780470015902.a0000584.pub3>.
- 572 [43] A. Biran, S. Yagur-Kroll, R. Pedahzur, S. Buchinger, G. Reifferscheid, H. Ben-Yoav,
573 Y. Shacham-Diamand, S. Belkin, Bacterial genotoxicity bioreporters, *Microb. Biotechnol.*
574 3 (4) (2010) 412–427. <https://doi.org/10.1111/j.1751-7915.2009.00160.x>.
- 575 [44] H. Ghodke, B.P. Paudel, J.S. Lewis, S. Jergic, K. Gopal, Z.J. Romero, E.A. Wood, R.
576 Woodgate, M.M. Cox, A.M. van Oijen, Spatial and temporal organization of RecA in the
577 *Escherichia coli* DNA-damage response, *BioRxiv.* 413880 (2018) 1–37.
578 <https://doi.org/10.7554/eLife.42761.025>.
- 579 [45] A. Lopreside, M.M. Calabretta, L. Montali, A. Roda, E. Michelini, Live Cell
580 Immobilization, in: G. Thouand (Ed.), *Handbook of Cell Biosensors*, Springer, Cham, 2019.
- 581 [46] E. Elcin, H.A. Öktem, Whole-cell fluorescent bacterial bioreporter for arsenic detection
582 in water, *Int. J. Environ. Sci. Technol.* 16 (2019) 5489–5500.
583 <https://doi.org/10.1007/s13762-018-2077-0>.
- 584 [47] H. Fukuda, M. Arai, K. Kuwajima, Folding of green fluorescent protein and the cycle3
585 mutant, *Biochemistry* 39 (2000) 12025–12032. <https://doi.org/10.1021/bi000543l>.
- 586 [48] E. Elcin, H.A. Öktem, Immobilization of fluorescent bacterial bioreporter for arsenic
587 detection, *J. Environ. Heal. Sci. Eng.* 18 (2020) 137–148. [https://doi.org/10.1007/s40201-](https://doi.org/10.1007/s40201-020-00447-2)
588 [020-00447-2](https://doi.org/10.1007/s40201-020-00447-2).
- 589 [49] X. Liu, Z. Guo, N.F. Roache, C.A. Mocka, M.R. Allen, M.A. Mason, Henry’s law
590 constant and overall mass transfer coefficient for formaldehyde emission from small water
591 pools under simulated indoor environmental conditions, *Environ. Sci. Technol.* 49 (2015)
592 1603–1610. <https://doi.org/10.1021/es504540c>.

- 593 [50] K.H. Maslowska, K. Makiela-Dzvenska, I.J. Fijalkowska, The SOS system: A complex
594 and tightly regulated response to DNA damage, *Environ. Mol. Mutagen.* 60 (2019) 368–
595 384. <https://doi.org/10.1002/em.22267>.
- 596 [51] L.R. Ptitsyn, G. Horneck, O. Komova, S. Kozubek, E.A. Krasavin, M. Bonev, P.
597 Rettberg, A biosensor for environmental genotoxin screening based on an SOS *lux* assay in
598 recombinant *Escherichia coli* cells, *Appl. Environ. Microbiol.* 63 (1997) 4377–4384.
599 <https://doi.org/10.1128/AEM.63.11.4377-4384.1997>.
- 600 [52] World Health Organization (WHO), Guidelines for drinking-water quality: Fourth
601 edition incorporating first addendum, ISBN 978-92-4-154995-0. Geneva, 2017.
- 602 [53] United States Environmental Protection Agency (US EPA), Edition of the Drinking
603 Water Standards and Health Advisories Tables EPA 822-F-18-001. Office of Water U.S.
604 Environmental Protection Agency Washington, DC, 2018.
- 605 [54] S. Bharadwaj, R.J. Mitchell, A. Qureshi, J.H. Niazi, Toxicity evaluation of e-juice and
606 its soluble aerosols generated by electronic cigarettes using recombinant bioluminescent
607 bacteria responsive to specific cellular damages, *Biosens. Bioelectron.* 90 (2017) 53–60.
608 <https://doi.org/10.1016/j.bios.2016.11.026>.
- 609 [55] B. Jiang, W.E. Huang, G. Li, Construction of a bioreporter by heterogeneously
610 expressing a: *Vibrio natriegens recA::luxCDABE* fusion in *Escherichia coli*, and
611 genotoxicity assessments of petrochemical-contaminated groundwater in northern China,
612 *Environ. Sci. Process. Impacts.* 18 (2016) 751–759. <https://doi.org/10.1039/c6em00120c>.
- 613 [56] M. kannan Maruthamuthu, V. Selvamani, G.T. Eom, S.H. Hong, Development of *recA*
614 promoter based bisphenol-A sensing and adsorption system by recombinant *Escherichia*
615 *coli*, *Biochem. Eng. J.* 122 (2017) 31–37. <https://doi.org/10.1016/j.bej.2017.02.009>.

- 616 [57] M. Matejczyk, W. Lewandowski, S.J. Rosochacki, *E. coli* K-12 *recA::gfp* microbial
617 biosensor used for screening of anticancer and antidiabetic pharmacist residues, *Desalin.*
618 *Water Treat.* 57 (2016) 1582–1592. <https://doi.org/10.1080/19443994.2014.996013>.
- 619 [58] J. Min, M.B. Gu, Genotoxicity assay using chromosomally-integrated bacterial *recA*:
620 *Lux*, *J. Microbiol. Biotechnol.* 13 (1) (2003) 99–103.
- 621 [59] R.J. Mitchell, M.B. Gu, An *Escherichia coli* biosensor capable of detecting both
622 genotoxic and oxidative damage, *Appl. Microbiol. Biotechnol.* 64 (2004) 46–52.
623 <https://doi.org/10.1007/s00253-003-1418-0>.
- 624 [60] Y. Song, G. Li, S.F. Thornton, I.P. Thompson, S.A. Banwart, D. N. Lerner, W.E. Huang,
625 Optimization of bacterial whole cell bioreporters for toxicity assay of environmental
626 samples, *Environ. Sci. Technol.* 43 (2009) 7931–7938. <https://doi.org/10.1021/es901349r>.
- 627 [61] G.J. Gao, L. Fan, H.M. Lu, Y.J. Hua, Engineering *Deinococcus radiodurans* into
628 biosensor to monitor radioactivity and genotoxicity in environment, *Chinese Sci. Bull.* 53
629 (2008) 1675–1681. <https://doi.org/10.1007/s11434-008-0224-6>.
- 630 [62] M. Kostrzynska, K.T. Leung, H. Lee, J.T. Trevors, Green fluorescent protein-based
631 biosensor for detecting SOS-inducing activity of genotoxic compounds, *J. Microbiol.*
632 *Methods.* 48 (2002) 43–51. [https://doi.org/10.1016/S0167-7012\(01\)00335-9](https://doi.org/10.1016/S0167-7012(01)00335-9).
- 633 [63] Y. Kuang, I. Biran, D.R. Walt, Living bacterial cell array for genotoxin monitoring,
634 *Anal. Chem.* 76 (2004) 2902–2909. <https://doi.org/10.1021/ac0354589>.
- 635 [64] M. Matejczyk, Specific for DNA damages GFP microbial biosensor as a tool for
636 genotoxic action assessment of environmental pollution, *Civil and Environmental*
637 *Engineering* (2010) 319–326.
- 638 [65] A. Norman, L.H. Hansen, S.J. Sørensen, Construction of a Cold *cda* promoter-based
639 SOS-green fluorescent protein whole-cell biosensor with higher sensitivity toward
640 genotoxic compounds than constructs based on *recA*, *umuDC*, or *sulA* promoters, *Appl.*

- 641 Environ. Microbiol. 71 (2005) 2338–2346. <https://doi.org/10.1128/AEM.71.5.2338->
642 2346.2005.
- 643 [66] M.S. Gangan, C.A. Athale, Threshold effect of growth rate on population variability of
644 *Escherichia coli* cell lengths, R. Soc. Open Sci. 4 (2) (2017) 160417.
645 <http://dx.doi.org/10.1098/rsos.160417>.
- 646 [67] S. Kamensšek, Z. Podlesek, O. Gillor, D. Žgur-Bertok, Genes regulated by the
647 *Escherichia coli* SOS repressor LexA exhibit heterogenous expression, BMC Microbiol. 10
648 (2010) 283. <https://doi.org/10.1186/1471-2180-10-283>.
- 649 [68] G.C. Gil, Y.J. Kim, M.B. Gu, Enhancement in the sensitivity of a gas biosensor by using
650 an advanced immobilization of a recombinant bioluminescent bacterium, Biosens.
651 Bioelectron. 17 (2002) 427–432. [https://doi.org/10.1016/S0956-5663\(01\)00305-0](https://doi.org/10.1016/S0956-5663(01)00305-0).
- 652 [69] N. Kováts, E. Horváth, Bioluminescence-based assays for assessing eco- and
653 genotoxicity of airborne emissions, Luminescence 31 (2016) 918–923.
654 <https://doi.org/10.1002/bio.3102>.
- 655 [70] B.-B. Lee, P. Ravindra, E.-S. Chan, Size and shape of calcium alginate beads produced
656 by extrusion dripping, Chem. Eng. Technol. 36 (10) (2013) 1627–1642.
657 <https://doi.org/10.1002/ceat.201300230>.
- 658 [71] J. Ma, B. Veltman, Z. Tietel, L. Tsrer, Y. Liu, E. Eltzov, Monitoring of infection volatile
659 markers using CMOS-based luminescent bioreporters, Talanta 219 (2020) 121333.
660 <https://doi.org/10.1016/j.talanta.2020.121333>.
- 661 [72] E. Eltzov, A. Yehuda, R.S. Marks, Creation of a new portable biosensor for water
662 toxicity determination, Sensors Actuators, B Chem. 221 (2015) 1044–1054.
663 <https://doi.org/10.1016/j.snb.2015.06.153>.
- 664 [73] T.-C. Tang, E. Tham, X. Liu, K. Yehl, A.J. Rovner, H. Yuk, C. de la Fuente-Nunez, F.J.
665 Isaacs, X. Zhao, T.K. Lu, Hydrogel-based biocontainment of bacteria for continuous

666 sensing and computation, Nat. Chem. Biol. (2021). [https://doi.org/10.1038/s41589-021-](https://doi.org/10.1038/s41589-021-00779-6)
667 00779-6.

668 [74] P. Sinharoy, S.L. McAllister, M. Vasu, E.R. Gross, Environmental Aldehyde Sources
669 and the Health Implications of Exposure, in: J. Ren, Y. Zhang, J. Ge (Eds.), Aldehyde
670 Dehydrogenases, Advances in Experimental Medicine and Biology, vol 1193. Springer,
671 Singapore, 2019, pp. 35-52.

672 [75] B.C. Campbell, E.M. Nabel, M.H. Murdock, C. Lao-Peregrin, P. Tsoufias, M.G.
673 Blackmore, F.S. Lee, C. Liston, H. Morishita, G.A. Petsko, mGreenLantern: a bright
674 monomeric fluorescent protein with rapid expression and cell filling properties for neuronal
675 imaging, Proc. Natl. Acad. Sci. USA 117 (2020) 30710–30721.
676 <https://doi.org/10.1073/pnas.2000942117>.

677 [76] P. Rugbjerg, C. Knuf, J. Förster, M.O.A. Sommer, Recombination-stable multimeric
678 green fluorescent protein for characterization of weak promoter outputs in *Saccharomyces*
679 *cerevisiae*, FEMS Yeast Res. 15 (2015) 1–8. <https://doi.org/10.1093/femsyr/fov085>.

680

681 **FIGURE LEGENDS**

682 **Fig. 1.** Complete map of formaldehyde sensor plasmid pBR-PrecA. Abbreviations used: *AmpR*,
683 confers resistance to ampicillin; *ori*, pBR322 origin of replication; *bom*, basis of motility; *rop*,
684 maintains plasmids at low copy number; *recAp*, DNA-damage responsive promoter; sGFP,
685 promoterless gene for green fluorescent protein.

686

687 **Fig. 2. a)** Growth curve of bioreporter cells treated with different formaldehyde concentrations
688 **b)** Fluorescence emission kinetics of FA bioreporter in response to different liquid
689 formaldehyde concentrations. The average of triplicate measurements is plotted with standard
690 deviations. Error bars are shown only when they exceed the size of the symbols **c)** Fluorescence
691 micrographs of uninduced and 500 μ M formaldehyde-induced bioreporter cells after 16-h
692 treatment. Scale bars are 100 μ m.

693

694 **Fig. 3.** Summary of experimental procedure describing formation of bioreporter immobilized
695 Ca-alginate hydrogel beads. The figure was created with BioRender.com.

696

697 **Fig. 4. a)** Fluorescence emission kinetics of alginate bead immobilized FA bioreporter in
698 response to different liquid formaldehyde concentrations. The average value of a triplicate of
699 each induction is presented with standard deviation. Error bars are shown only when they
700 exceed the size of the symbols **b)** The photo of uninduced and induced (with liquid 500 μ M
701 FA) beads. Images were taken by smartphone camera while the beads were placed on EVOS
702 Fluid Imaging Station (Thermo Fisher Scientific, USA) using blue excitation (390 ± 40 nm)
703 with emission detection at 446 ± 33 nm.

704

705 **Fig. 5.** Overview of the basic experimental procedure of gaseous formaldehyde detection. The
706 figure was created with BioRender.com.

707

708 **Fig. 6.** Effect of bead assay solutions on the gaseous FA detection performances of alginate-
709 immobilized FA bioreporter. The average value from triplicates of each induction is presented
710 for 16-h assay time with standard deviation.

711

712 **Fig. 7.** Fluorescence emission kinetics of alginate bead immobilized FA bioreporter in response
713 to different gaseous formaldehyde concentrations assayed in **a)** MSSM and **b)** 0.5X MSSM.
714 The average value of a triplicate of each induction is presented with standard deviation. Error
715 bars are shown only when they exceed the size of the symbols.

716

717 **Fig. 8.** Gaseous selectivity of the FA bacterial bioreporter assayed in the MSSM and 0.5X
718 MSSM. The gas concentrations of FA and other VOCs were at 400 μ M. Measurements were
719 performed following 16-h treatment.

FIGURES

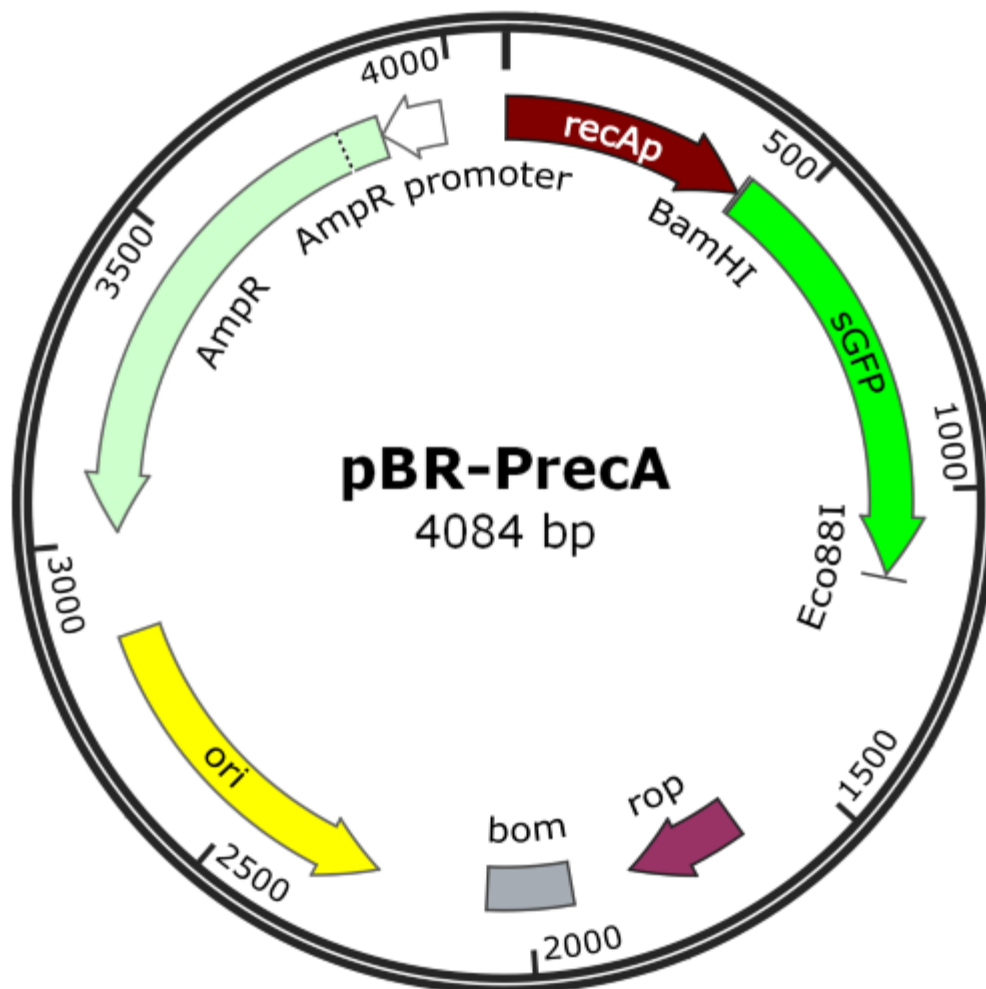


FIGURE 1

Fig. 1. Complete map of formaldehyde sensor plasmid pBR-PrecA. Abbreviations used: *AmpR*, confers resistance to ampicillin; *ori*, pBR322 origin of replication; *bom*, basis of motility; *rop*, maintains plasmids at low copy number; *recAp*, DNA-damage responsive promoter; sGFP, promoterless gene for green fluorescent protein.

FIGURE 2a

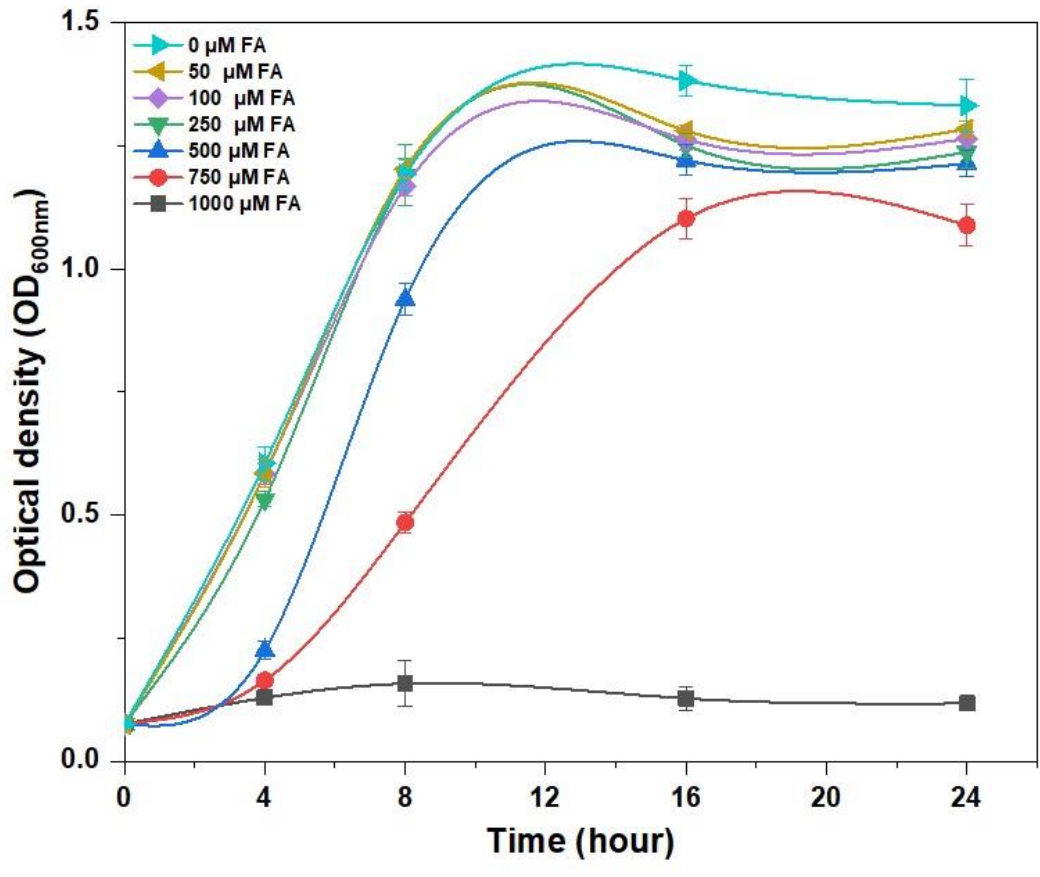


FIGURE 2b

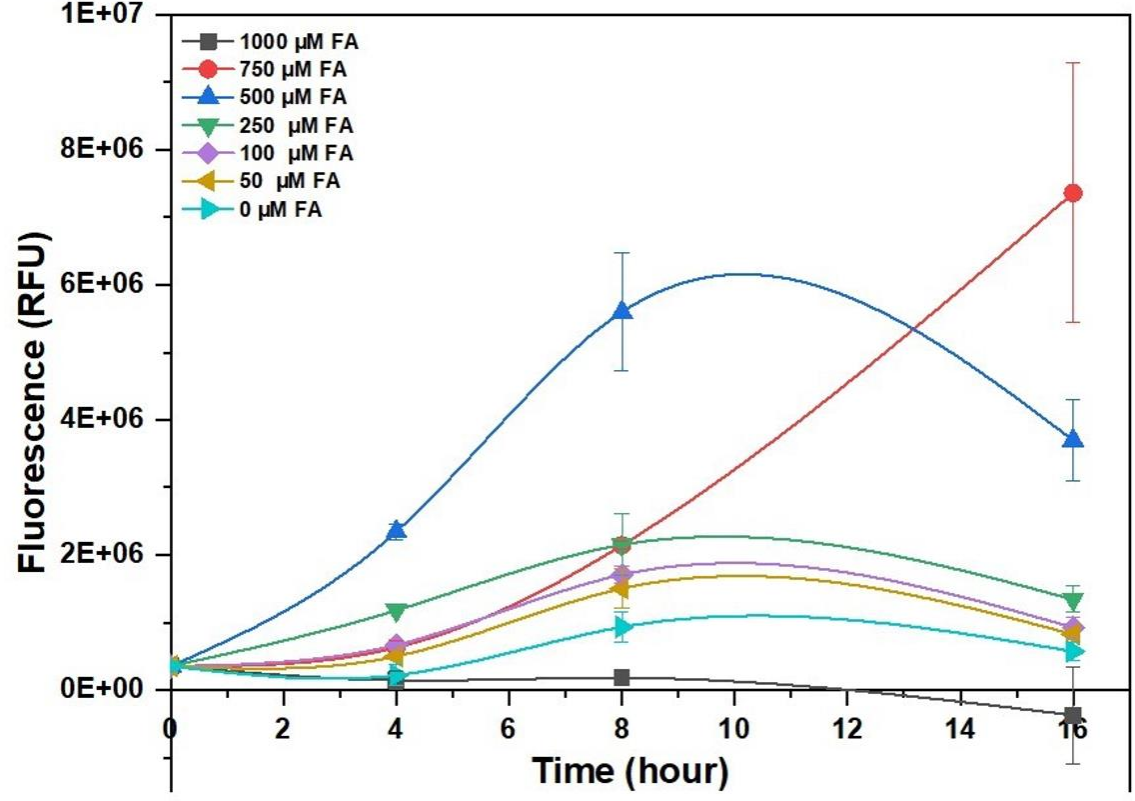


FIGURE 2c

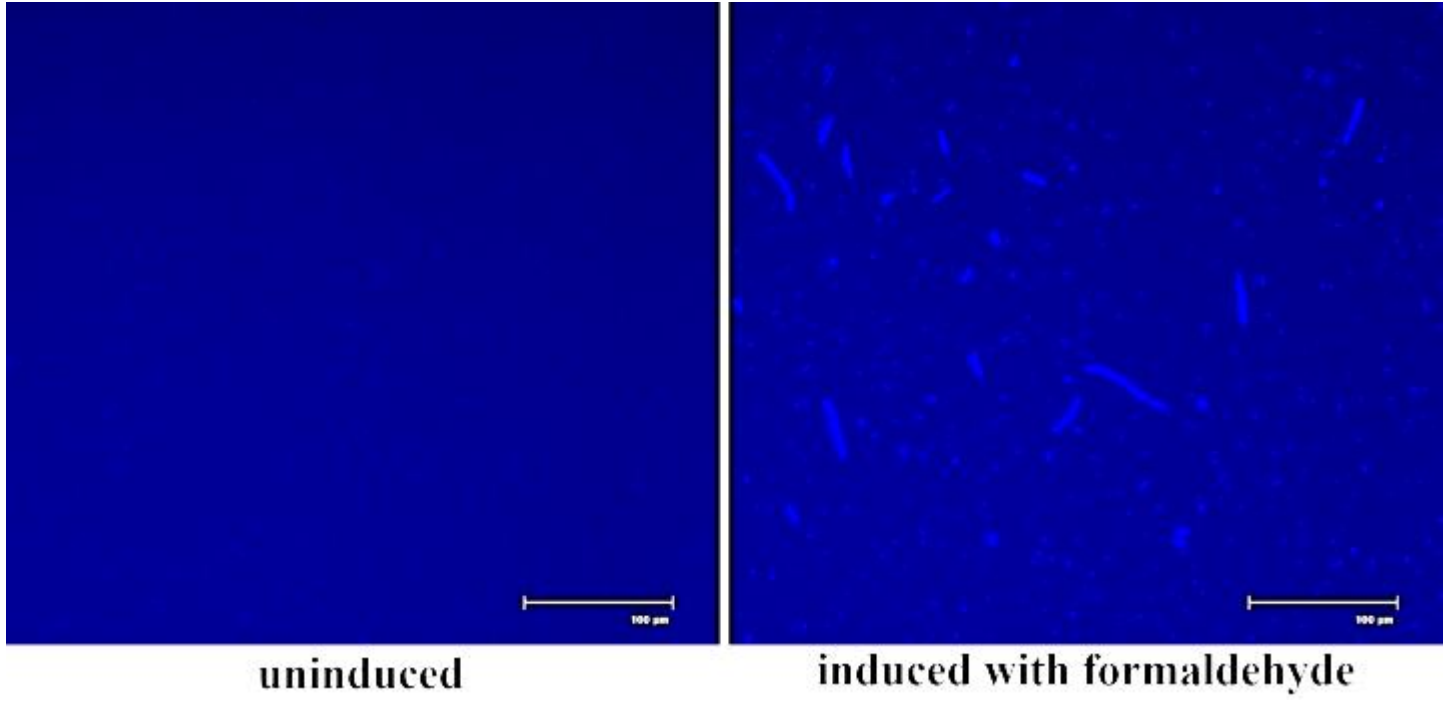


Fig. 2. a) Growth curve of bioreporter cells treated with different formaldehyde concentrations **b)** Fluorescence emission kinetics of FA bioreporter in response to different liquid formaldehyde concentrations. The average of triplicate measurements is plotted with standard deviations. Error bars are shown only when they exceed the size of the symbols **c)** Fluorescence micrographs of uninduced and 500 μM formaldehyde-induced bioreporter cells after 16-h treatment. Scale bars are 100 μm.

FIGURE 3

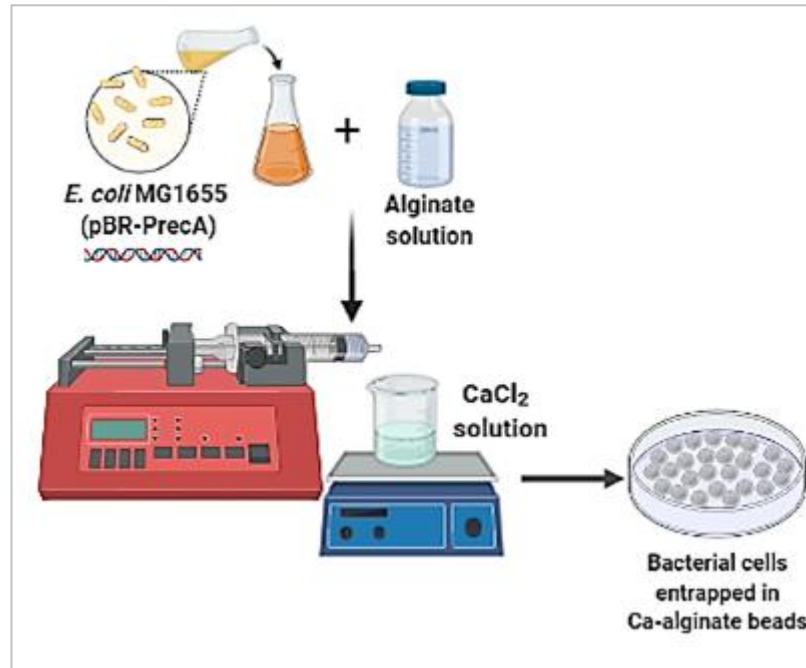


Fig. 3. Summary of experimental procedure describing formation of bioreporter immobilized Ca-alginate hydrogel beads. The figure was created with BioRender.com.

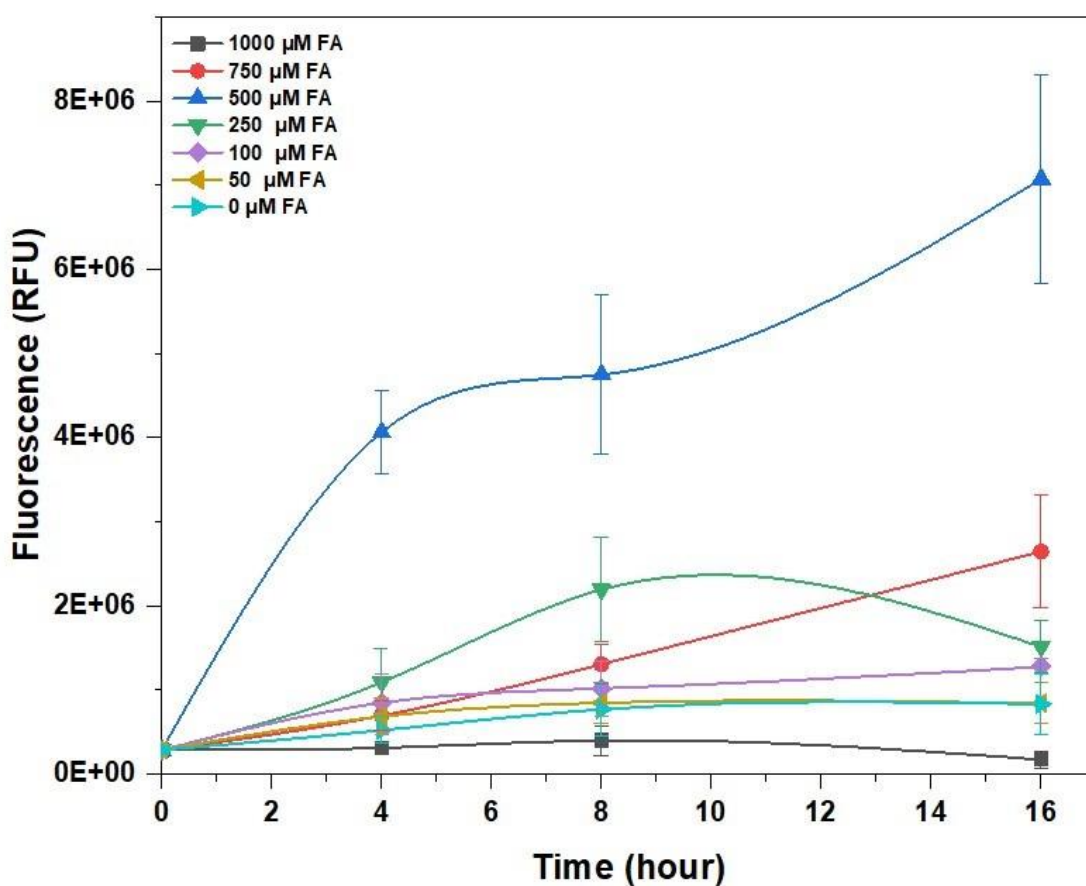


FIGURE 4a

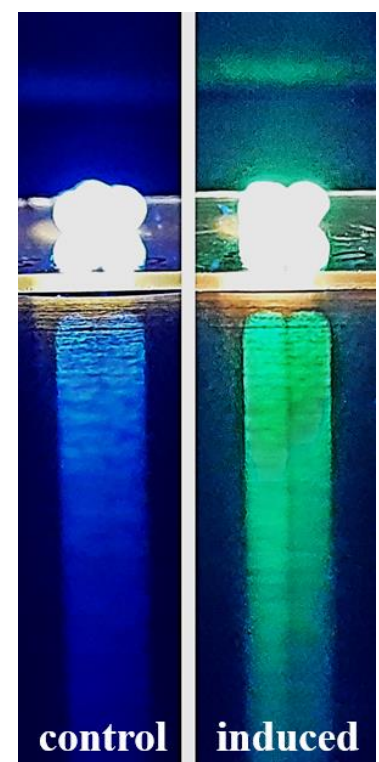


FIGURE 4b

Fig. 4. a) Fluorescence emission kinetics of alginate bead immobilized FA bioreporter in response to different liquid formaldehyde concentrations. The average value of a triplicate of each induction is presented with standard deviation. Error bars are shown only when they exceed the size of the symbols **b)** The photo of uninduced and induced (with liquid 500 μM FA) beads. Images were taken by smartphone camera while the beads were placed on EVOS Fluid Imaging Station (Thermo Fisher Scientific, USA) using blue excitation (390 ± 40 nm) with emission detection at 446 ± 33 nm.

FIGURE 5

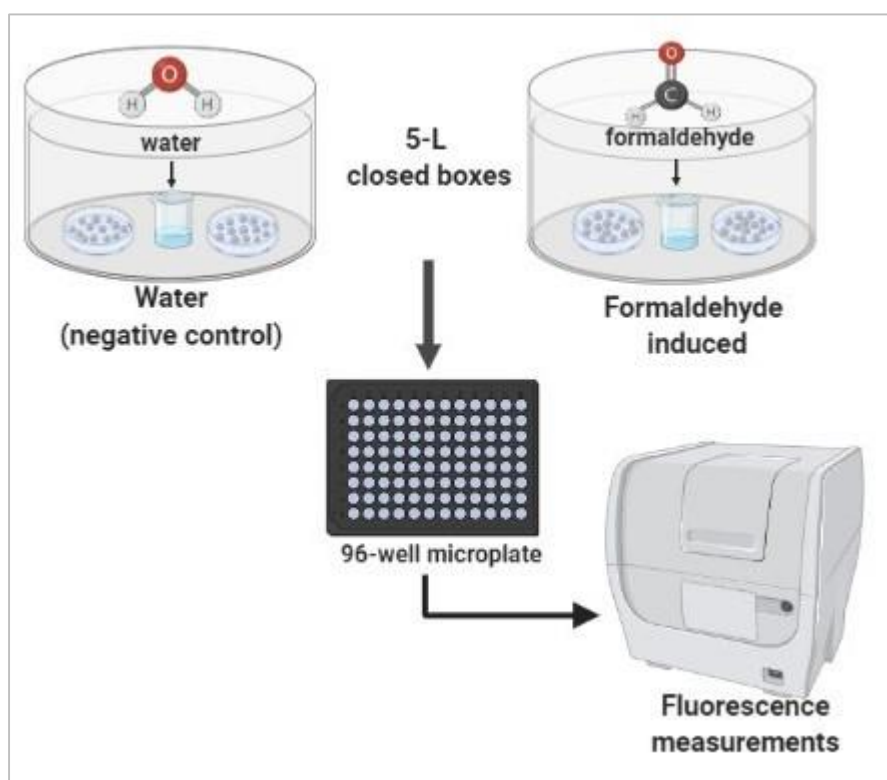


Fig. 5. Overview of the basic experimental procedure of gaseous formaldehyde detection. The figure was created with BioRender.com.

FIGURE 6

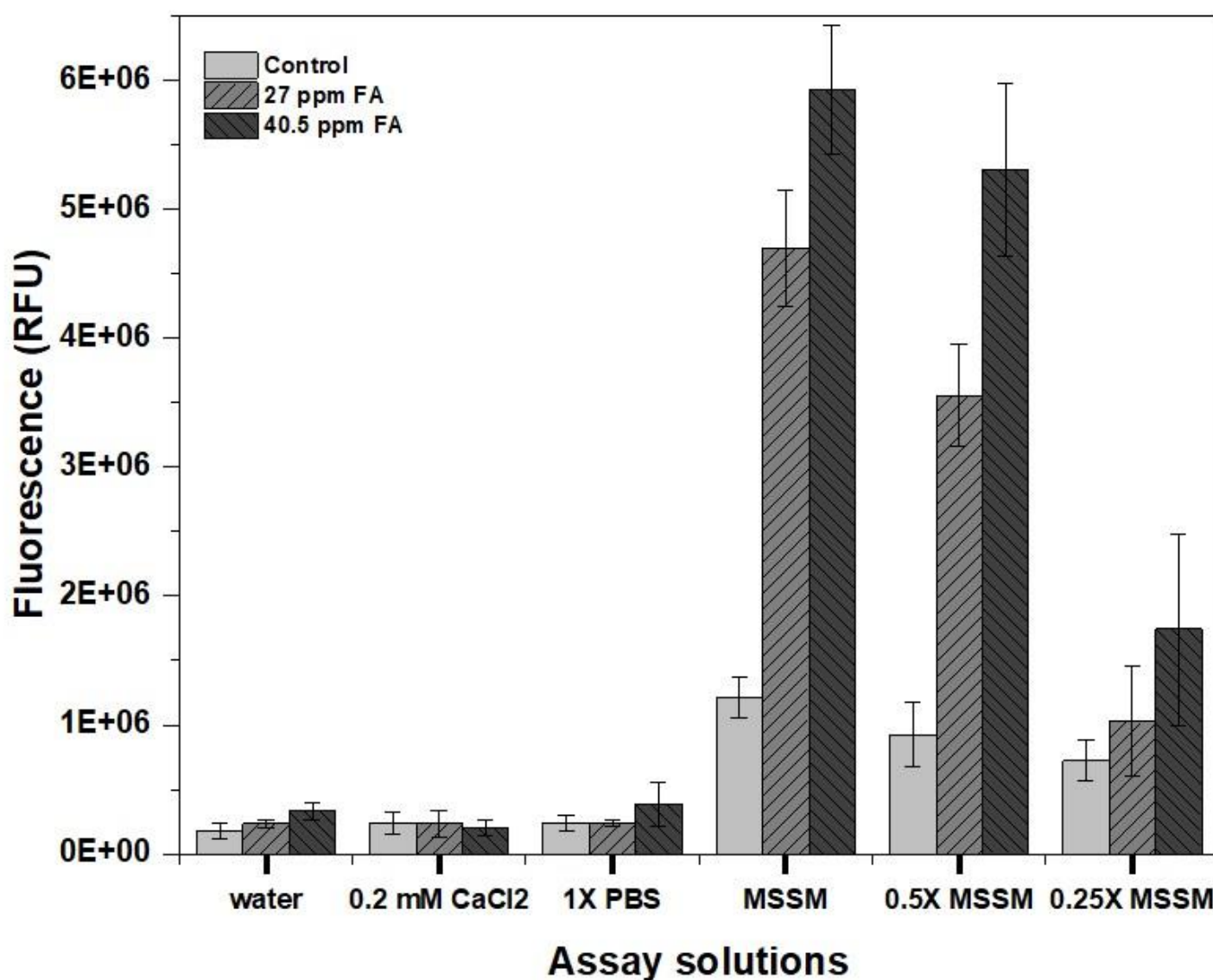


Fig. 6. Effect of bead assay solutions on the gaseous FA detection performances of alginate-immobilized FA bioreporter. The average value from triplicates of each induction is presented for 16-h assay time with standard deviation.

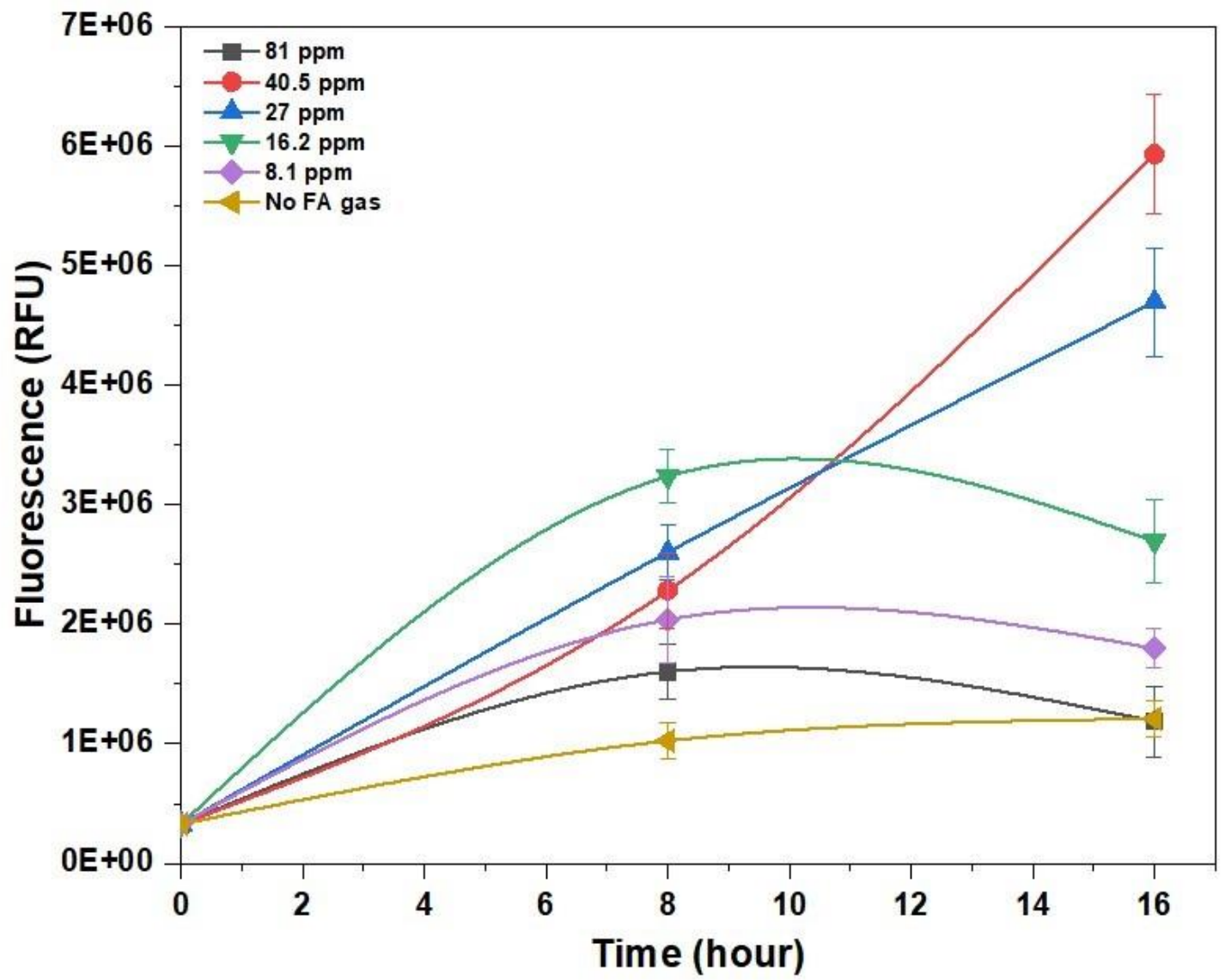


FIGURE 7a

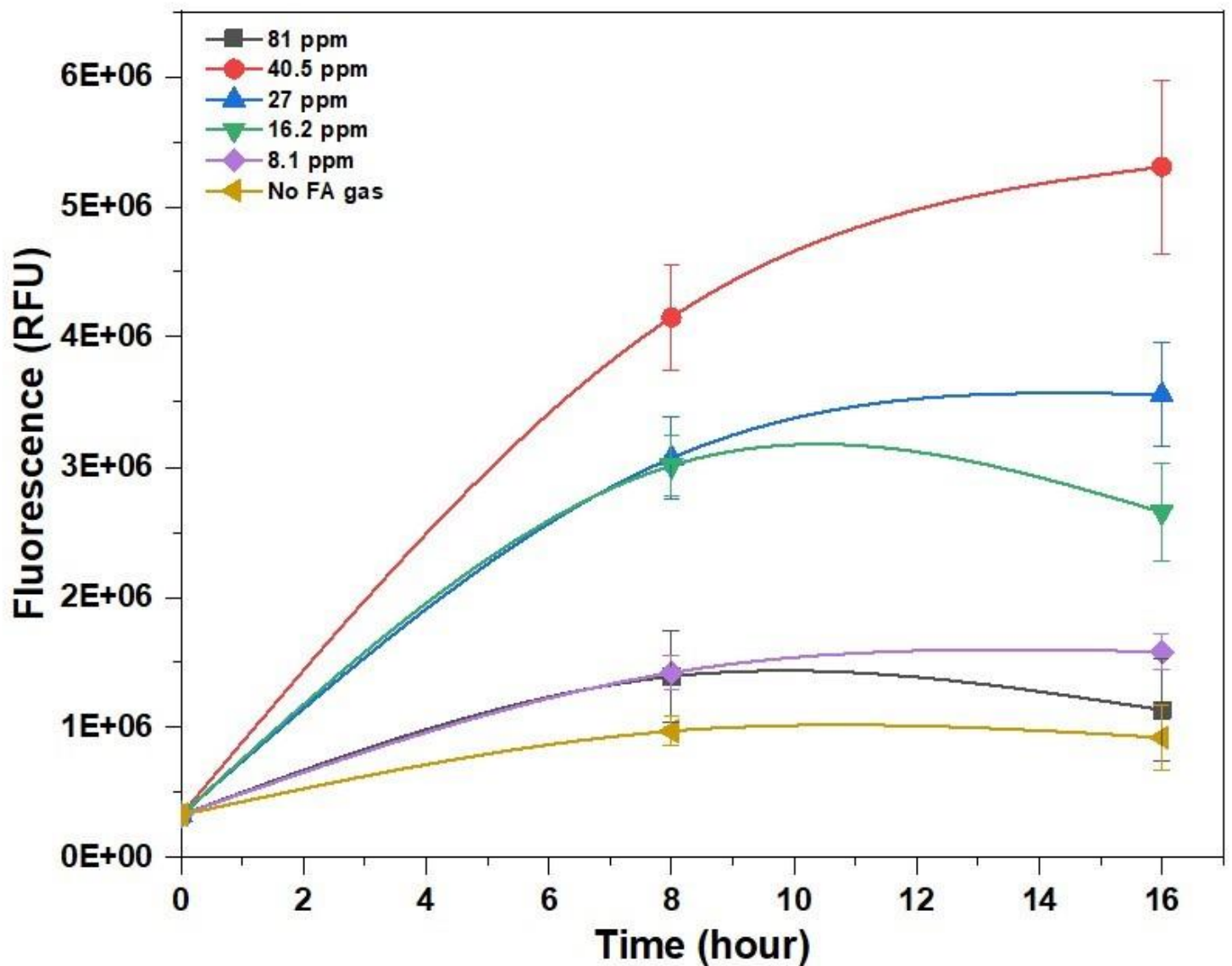


FIGURE 7b

Fig. 7. Fluorescence emission kinetics of alginate bead immobilized FA bioreporter in response to different gaseous formaldehyde concentrations assayed in **a)** MSSM and **b)** 0.5X MSSM. The average value of a triplicate of each induction is presented with standard deviation. Error bars are shown only when they exceed the size of the symbols.

FIGURE 8

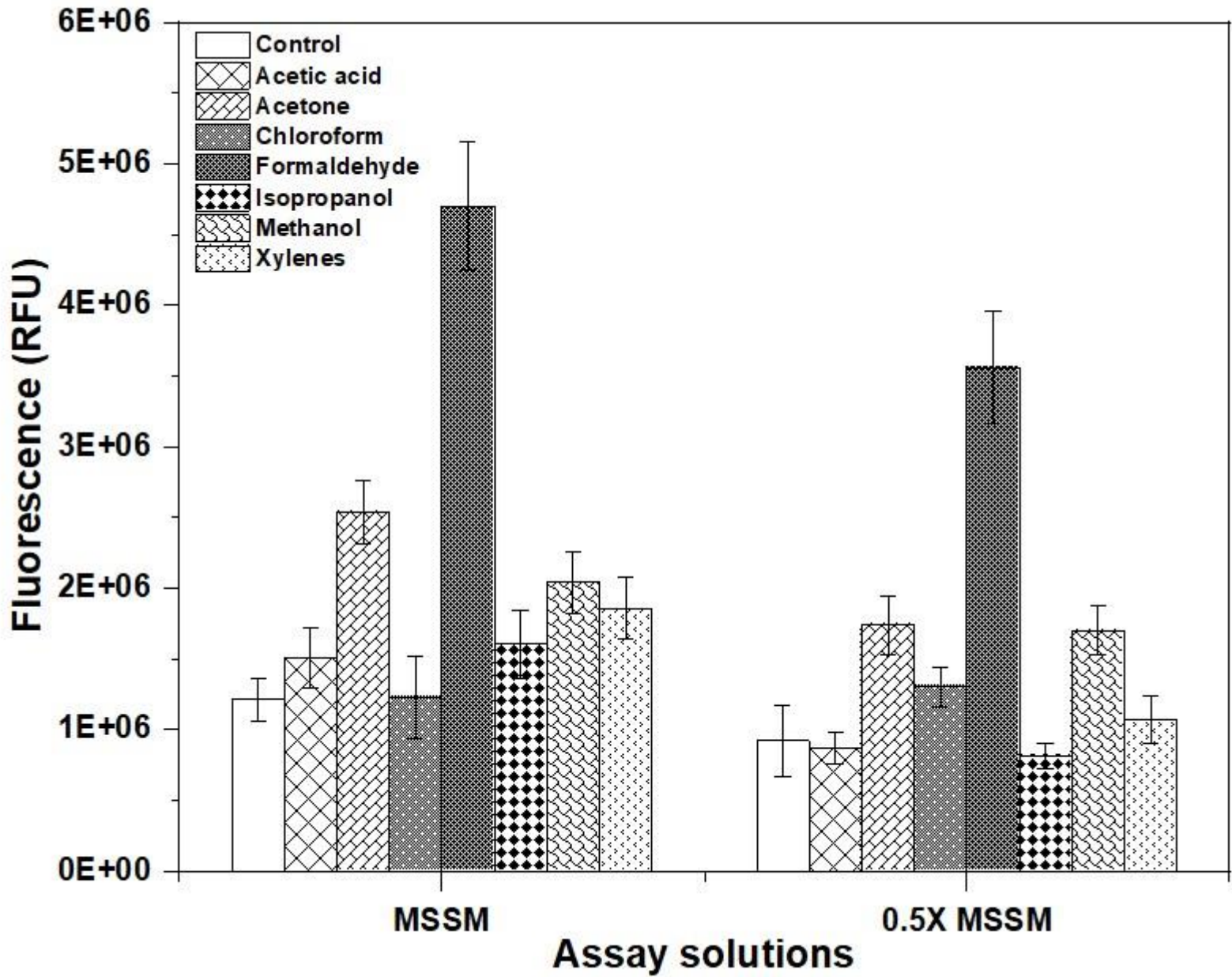


Fig. 8. Gaseous selectivity of the FA bacterial bioreporter assayed in the MSSM and 0.5X MSSM. The gas concentrations of FA and other VOCs were at 400 μ M. Measurements were performed following 16-h treatment.